Research Square

Preprints are preliminary reports that have not undergone peer review.
They should not be considered conclusive, used to inform clinical practice,
or referenced by the media as validated information.

Disease-duration-associated ALPS asymmetry in migraine: a case-control DTI-ALPS study

Liang Dong
The First Affiliated Hospital of Chongqing Medical University
Wanqun Hu
The First Affiliated Hospital of Chongqing Medical University
Linyi Che
The First Affiliated Hospital of Chongqing Medical University
Qinlian Huang
The First Affiliated Hospital of Chongqing Medical University
Yuhui Xu
The First Affiliated Hospital of Chongqing Medical University
Siyan Luo
The First Affiliated Hospital of Chongqing Medical University
Hui Li
The First Affiliated Hospital of Chongqing Medical University
Ge Tan
The First Affiliated Hospital of Chongqing Medical University
Xiaoping Fan
The First Affiliated Hospital of Chongqing Medical University
Jiying Zhou
zhoujiying@hospital.cqmu.edu.cn

The First Affiliated Hospital of Chongqing Medical University

---

Research Article

Keywords: ALPS, putative glymphatic function, migraine, disease duration, acute medication days, MRI, laterality

Posted Date: June 30th, 2026

DOI: https://doi.org/10.21203/rs.3.rs-10111118/v1

License: This work is licensed under a Creative Commons Attribution 4.0 International License.
Read Full License

Additional Declarations: No competing interests reported.

Abstract

Background

Migraine ALPS studies have reported mixed case-control findings. Because averaging hemispheres may obscure clinically relevant laterality, we tested whether hemisphere-specific ALPS variation showed patient-internal associations with disease duration beyond the pooled case-control contrast, and secondarily whether baseline hemisphere-specific ALPS was associated with later acute medication use.

Methods

We analyzed 89 participants (25 controls, 64 migraine patients) recruited between December 2021 and June 2023. Bilateral ALPS was tested with age-, sex-, and BMI-adjusted Gaussian GEE. In patients, disease duration was related to left, right, mean, right-minus-left, and absolute-difference ALPS metrics in five FDR-controlled HC3-robust models adjusted for baseline MMD, age, sex, and BMI, plus a baseline-MMD-adjusted hemisphere-aware GEE. A secondary two-model family examined left and right baseline ALPS in relation to follow-up acute medication days (AMD) assessed in February 2026, adjusting for baseline AMD, baseline MMD, disease duration, age, sex, and BMI.

Results

Case-control status was not associated with ALPS. Right-hemisphere ALPS was lower than left in the bilateral GEE (β=-0.0653, 95% CI -0.1149 to -0.0156, p = 0.010), without a patient-by-side interaction. Within the migraine cohort, longer duration was associated with higher right-minus-left ALPS difference (β = 0.0053, p = 0.003, FDR-corrected p = 0.015) and lower absolute ALPS difference (β=-0.0037, p = 0.006, FDR-corrected p = 0.016) after baseline-MMD adjustment; the left-ALPS slope was nominal only (FDR-corrected p = 0.076). Hemisphere-aware GEE showed a side-by-duration interaction (p < 0.001). Higher baseline left ALPS was associated with follow-up AMD in the secondary two-model family after adjustment for baseline AMD, baseline MMD, disease duration, age, sex, and BMI (β = 1.2874, p = 0.014, FDR-corrected p = 0.029).

Conclusions

Hemisphere-specific ALPS metrics revealed disease-duration associations not captured by pooled case-control status. The main signal was a less leftward ALPS asymmetry pattern at longer disease duration, whereas the follow-up AMD association remains secondary and exploratory. Prospective studies should pair ALPS laterality with synchronized clinical windows, diary-based medication-use assessment, and lateralization phenotyping.

Trial registration

Not applicable.

Background

The glymphatic system has been proposed as a brain-wide perivascular transport pathway involved in fluid homeostasis and waste clearance, and diffusion tensor image analysis along the perivascular space (DTI-ALPS) was introduced as a non-invasive MRI-derived index to interrogate this biology in vivo [1–2]. Although ALPS is attractive because it can be obtained retrospectively from standard diffusion acquisitions, recent methodological work has emphasized that the metric reflects a mixture of perivascular diffusivity, white matter geometry, and acquisition-dependent factors rather than a direct readout of glymphatic flow [2–5].

Interest in putative glymphatic involvement in headache disorders has risen quickly. Reviews have highlighted plausible links between headache pathophysiology and glymphatic or related fluid-clearance pathways [6–7]. Yet migraine imaging studies using ALPS-related metrics remain heterogeneous: some reported little or no case-control separation [8], whereas others described higher ALPS in chronification [9], altered DKI-ALPS metrics [10], or impaired putative glymphatic and meningeal lymphatic function in chronic migraine [11]. More recent work has also linked meningeal lymphatic drainage, glymphatic dysfunction in high-frequency episodic migraine, and sleep-related variation to migraine burden [12–14].

One plausible explanation for these mixed findings is methodological. Many studies summarize ALPS by pooling hemispheres or relying on average or unilateral metrics, a strategy that may obscure biologically relevant asymmetry. This concern is especially relevant in migraine, where clinical lateralization is common and left- versus right-sided phenotypes may differ across several domains [15]. A more recent cross-sectional study likewise reported higher headache burden in patients with typically left-sided versus right-sided migraine, reinforcing the possibility that sidedness captures clinically meaningful variation rather than simple noise [16].

Migraine is also heterogeneous in burden and biology, and current diagnostic criteria do not fully capture that heterogeneity [17]. Broader epidemiologic work further shows that migraine burden extends beyond attack frequency to disability, psychiatric and medical comorbidity, healthcare use, and quality of life [18]. EM, CM, and VM differ in frequency, symptom profile, and treatment needs, yet subtype labels may not fully capture continuous clinical variation. These considerations make disease duration and hemisphere-specific modeling useful for testing whether ALPS variation shows patient-internal structure beyond a simple patient-versus-control shift.

We therefore tested whether hemisphere-specific ALPS patterns showed patient-internal associations with disease duration that were not apparent in a pooled case-control contrast. We also examined, as a secondary analysis, whether baseline left and right ALPS were associated with later acute medication use assessed in February 2026.

Methods

Study design and participants

This was a single-center cross-sectional case-control analysis of a clinical-imaging dataset containing demographic, clinical, and bilateral ALPS variables from 89 participants with usable ALPS values. This cross-sectional case-control analysis is reported in accordance with the STROBE guidelines [19]; a completed checklist is provided as Supplementary Checklist S1. Participants were recruited between December 2021 and June 2023 from the headache clinic of the First Affiliated Hospital of Chongqing Medical University, Chongqing, China. Healthy controls with no history of headache were recruited to be frequency-matched to the patient group by age and sex. Diagnostic code 0 identified healthy controls (n = 25). Codes 1–3 identified episodic migraine (EM; n = 20), chronic migraine (CM; n = 24), and vestibular migraine (VM; n = 20), respectively. All 64 patients had subtype labels and complete covariate data for the patient-only models. Because two controls lacked BMI, the BMI-adjusted case-control GEE used 87 complete cases.

Migraine inclusion criteria were age 18–60 years, ability to understand and sign written informed consent, fulfillment of ICHD-3 diagnostic criteria for EM, CM, or VM [20], at least 1 year of migraine history, migraine onset before 50 years of age, ability and willingness to complete questionnaires, willingness to keep a headache diary during the study period, and good protocol adherence. In the source cohort, the EM arm was restricted to patients meeting ICHD-3 criteria for migraine without aura. Migraine diagnoses and subtype assignments were adjudicated according to ICHD-3 by two headache specialists.

Migraine exclusion criteria were other chronic pain or sensory disorders, history of head trauma, intracranial disease or surgery, current or past major psychiatric illness (including bipolar disorder, schizophrenia, personality disorder, or other severe mood or anxiety disorder), uncontrolled diabetes (glycated hemoglobin > 8.0) or diabetic complications, uncontrolled hypertension (> 150/95 mmHg at screening), acute severe or unstable medical illness, other neurologic disease, abnormal cranial imaging findings (for example intracranial space-occupying lesions), acute or rescue medication use within 24 hours before MRI, use within 12 hours before MRI of sedatives, hypnotics, coffee, strong tea, alcohol, or other exposures likely to affect study results, pregnancy or lactation, substance or alcohol abuse/dependence, MRI contraindications, or investigator judgment of unsuitability.

Healthy-control inclusion criteria were age 18–60 years, ability to understand and sign written informed consent, no lifetime history of any headache disorder, no clinically evident depression or anxiety, and good general mental status. Healthy-control exclusion criteria were any headache history or other chronic pain syndrome, uncontrolled diabetes or hypertension, substance or alcohol abuse/dependence, psychiatric illness, neurologic disease, pregnancy or lactation, acute severe or unstable medical illness, prior head trauma, inability to cooperate with testing, MRI contraindications, use within 12 hours before

MRI of analgesics, sedatives, hypnotics, coffee, strong tea, alcohol, or other exposures likely to affect study results, or investigator judgment of unsuitability.

The study was approved by the Ethics Committee of the First Affiliated Hospital of Chongqing Medical University (approval No. CY2020-594). All participants provided written informed consent before enrollment and MRI examination.The present secondary analysis was additionally approved by the same Ethics Committee (approval No. 2026-0375-01).

MRI preparation, acquisition, and DTI-ALPS processing

To reduce scan-state confounding, MRI timing was handled according to migraine subtype. For patients with episodic migraine without aura or vestibular migraine, scanning was scheduled outside headache and vertigo attacks: no headache or vertigo attack was allowed within 24 hours before MRI, and the same 24-hour post-scan window was checked by telephone. If headache or vertigo occurred within this peri-scan window, the participant was recalled for repeat MRI at a later date or the scan was excluded if repeat scanning was not possible. For patients with chronic migraine, complete pain freedom was not required; scans were accepted in a pain-free state or with mild background headache, but not during clinically significant acute worsening. Specifically, patients with chronic migraine were not scanned if they had ongoing moderate-to-severe headache on the scan day, defined as an NRS score of 4 or higher, clinically significant headache worsening within the preceding 24 hours, or rescue medication use within the preceding 24 hours.

Participants were instructed on the day before MRI to avoid beverages or foods that might alter neural activity, including coffee, tea, and alcohol. All metallic objects and electronic devices were removed, metallic implants were excluded, and MRI examination consent was obtained before scanning. During MRI, participants lay supine with eyes closed. A head-fixation device was used to reduce motion, earplugs were provided for noise reduction, and participants were instructed to remain relaxed, minimize body movement, and stay awake. Immediately after MRI, participants were asked whether they had slept or experienced headache during the examination. Patients with chronic migraine were contacted by telephone 24 hours after MRI to ask about clinically significant headache worsening or rescue medication use; if either occurred, repeat MRI at a later date was arranged or the scan was excluded. Image quality was reviewed by the MRI technologist; scans not meeting quality requirements were repeated or excluded. Before the final analytical dataset was locked, 2 participants underwent repeat MRI under the peri-scan criteria, 3 participants were excluded under the peri-scan criteria, and 3 scans were excluded for image-quality failure. Registration outputs and template-space ROI overlays were visually reviewed for gross misregistration or out-of-brain ROI placement before diffusivity extraction. Healthy controls underwent one MRI examination using the same acquisition protocol.

MRI was performed on a Philips Ingenia DNA 3.0-T scanner using a 32-channel head coil. Diffusion-weighted images were acquired with a single-shot spin-echo echo-planar imaging (SS-SE-EPI) sequence. Acquisition parameters were repetition time (TR) 2435 ms, echo time (TE) 88 ms, flip angle 90°, field of

view 224 × 224 mm, matrix 112 × 112, 72 slices, slice thickness 2.0 mm with no interslice gap, isotropic voxel size 2.0 × 2.0 × 2.0 mm3, number of excitations 1, b value 1000 s/mm2, one b0 image, and 128 diffusion-encoding directions; scan time was approximately 5 min 19 s.

DTI-ALPS processing followed the approach proposed by Taoka and colleagues [1–3]. Raw DICOM data were converted to NIfTI format with MRIcroGL. Preprocessing used FSL, MRtrix3 (version 3.0.4), and Advanced Normalization Tools (ANTs). DTI images were denoised with the MRtrix3 dwidenoise command to suppress Gaussian noise, followed by MRtrix3 Gibbs-ringing correction. Head-motion and eddy-current correction were performed with dwifslpreproc, and N4 bias-field correction was applied with ANTs. Non-brain tissue was removed with the FSL BET2 pipeline, yielding the B0 image and brain mask. Diffusion-tensor fitting was performed with the FSL dtifit command, from which FA, color-coded FA, tensor maps, and directional diffusivity maps were derived, including Dxx, Dyy, and Dzz.

Each participant's FA map was linearly registered with FSL FLIRT to the JHU-ICBM-FA-1mm template, and the same transformation was applied to the Dxx, Dyy, and Dzz maps. Following the standard ALPS workflow, spherical ROIs with a 5-mm radius were placed in template space in the projection and association fiber regions: left superior corona radiata (116, 110, 99), left superior longitudinal fasciculus (128, 110, 99), right superior corona radiata (64, 110, 99), and right superior longitudinal fasciculus (51, 110, 99). Diffusivities along the x-, y-, and z-axes were extracted from each ROI. This fixed template-space ROI strategy was used to reduce operator-dependent variability in ROI placement. The ALPS index was calculated as mean(Dxxproj, Dxxassoc) / mean(Dyyproj, Dzzassoc). The processing route and template-space ROI placement are summarized in Fig. 1.

Clinical variables and ALPS metrics

The ALPS-derived outcomes available in the extract were left ALPS, right ALPS, ALPS difference (defined in the source sheet as right minus left), absolute ALPS difference, and mean ALPS. Disease duration was analyzed as the primary patient-level duration variable for the main patient-cohort question.

The source dataset defined MMD as monthly migraine days. Patients were instructed to maintain headache diaries during the study. The de-identified analytical extract retained baseline AMD, follow-up AMD, baseline MMD, a source-field variable labeled current MMD, MIDAS, HIT-6, HADS, DHI, VSS, headache-location fields, and ever preventive-treatment history. Baseline MMD was anchored to the baseline clinical assessment and was included in the primary patient-only models; current MMD is reported descriptively only because its exact timing relative to MRI was unavailable. Follow-up AMD was obtained for all 64 patients through structured telephone follow-up in February 2026. Baseline MRI had been acquired between December 2021 and June 2023, corresponding to an imaging-to-follow-up interval of approximately 32–50 months. Follow-up AMD was treated as a later medication-use outcome, with baseline AMD retained as a covariate.

Statistical analysis

Continuous variables are summarized as mean ± standard deviation (SD) or median where appropriate; categorical variables are presented as counts and percentages. Healthy controls and the pooled patient cohort were compared with Welch's t test for continuous variables and Fisher's exact test for binary variables. Because ALPS metrics were primary outcomes, their unadjusted Table 1 comparisons are presented for descriptive context only, whereas adjusted case-control inference is based on the GEE models reported in Table 2.

Table 1
Baseline characteristics and patient clinical descriptors by case-control group

Variable	Healthy control (n = 25)	Patient cohort (n = 64)	Descriptive P
Participants, n	25	64	-
Age, years	36.20 ± 9.16	36.84 ± 9.52	0.770
Male sex, n (%)	6 (24.0)	5 (7.8)	0.067
BMI, kg/m²	22.36 ± 1.53	21.55 ± 2.44	0.074
Left ALPS	1.535 ± 0.146	1.553 ± 0.142	0.601
Right ALPS	1.459 ± 0.132	1.487 ± 0.119	0.376
ALPS difference (right-left)	-0.075 ± 0.127	-0.066 ± 0.132	0.764
Absolute ALPS difference	0.116 ± 0.089	0.102 ± 0.106	0.512
Mean ALPS	1.497 ± 0.124	1.520 ± 0.113	0.434
Disease duration, years	-	16.0 ± 9.7	-
Baseline MMD	-	10.0 ± 8.6	-
Baseline AMD	-	6.1 ± 7.5	-
Follow-up AMD (February 2026)	-	3.4 ± 4.8	-
Current MMD (source-field label)	-	6.2 ± 6.7	-
MIDAS total	-	24.3 ± 33.1	-
HIT-6 total	-	59.0 ± 11.3	-
HADS total	-	18.4 ± 10.5	-
DHI total	-	30.9 ± 24.6	-

Legend: Values are mean ± SD unless otherwise indicated. "Descriptive P" values compare healthy controls with the pooled migraine patient cohort using Welch's t test for continuous variables and Fisher's exact test for binary variables. ALPS metrics are displayed descriptively only; adjusted case-control inference is presented in Table 2. Follow-up AMD was assessed by structured telephone follow-up in February 2026. The source extract also retained a field labeled current MMD, shown descriptively only because its exact timing relative to MRI was unavailable. Headache-side labels were partly retained and are therefore reported descriptively rather than used for laterality inference.

Variable	Healthy control (n = 25)	Patient cohort (n = 64)	Descriptive P
VSS total	-	23.8 ± 21.2	-
Ever preventive treatment, n (%)	-	34 (53.1)	-
Unilateral headache location, n (%)	-	45 (70.3)	-
Detailed headache-side labels, n	-	left/right/bilateral/alternating/not retained = 10 / 7 / 12 / 5 / 30	-
Migraine subtype (EM/CM/VM), n	-	20 / 24 / 20	-

Legend: Values are mean ± SD unless otherwise indicated. "Descriptive P" values compare healthy controls with the pooled migraine patient cohort using Welch's t test for continuous variables and Fisher's exact test for binary variables. ALPS metrics are displayed descriptively only; adjusted case-control inference is presented in Table 2. Follow-up AMD was assessed by structured telephone follow-up in February 2026. The source extract also retained a field labeled current MMD, shown descriptively only because its exact timing relative to MRI was unavailable. Headache-side labels were partly retained and are therefore reported descriptively rather than used for laterality inference.

Table 2
Case-control GEE for bilateral ALPS

Term	β	95% CI low	95% CI high	P
Patient cohort (vs control)	0.023	-0.046	0.092	0.515
Right hemisphere (vs left)	-0.065	-0.115	-0.016	0.010
Patient × right hemisphere	-0.001	-0.060	0.058	0.979
Age, per year	-0.003	-0.007	0.000	0.084
Male sex	0.006	-0.060	0.072	0.861
BMI, kg/m²	0.003	-0.013	0.018	0.734

Legend: Gaussian GEE with exchangeable working correlation across bilateral ALPS observations. Healthy control and left hemisphere were the reference categories. Complete-case n = 87 because BMI was missing in two participants. The group term represents the left-sided patient-control contrast; the interaction term tests whether the patient-control contrast differs by hemisphere.

Derived contrasts from the GEE: right versus left among controls, estimate − 0.0653 (95% CI -0.1149 to -0.0156; p = 0.010); right versus left among patients, estimate − 0.0661 (95% CI -0.0981 to -0.0341; p < 0.001); patient versus control on the left, p = 0.515; patient versus control on the right, p = 0.484.

Case-control inference for ALPS was performed with a Gaussian generalized estimating equation (GEE) model in long format, with hemisphere treated as a repeated within-participant factor: ALPS ~ group + side + group×side + age + sex + BMI. This framework was chosen because each participant contributed

bilateral ALPS values and controls did not have disease duration or AMD values suitable for within-group clinical modeling.

Within the migraine cohort, baseline ALPS outcomes included left ALPS, right ALPS, mean ALPS, ALPS difference (right-left), and absolute ALPS difference. Because the patient-internal duration question was expected to be lateralized, left ALPS and the asymmetry metrics were treated as complementary duration-sensitive expressions of one laterality construct, with mean and right ALPS retained in the same FDR-controlled panel for completeness. To account for multiplicity across these five baseline outcomes, Benjamini-Hochberg false discovery rate (FDR) adjustment was applied within the disease-duration panel. Disease-duration associations that did not survive FDR were interpreted as nominal only.

A patient-only hemisphere-aware GEE model with a side-by-duration interaction (ALPS ~ side + duration + side × duration + baseline MMD + age + sex + BMI) was then used to test whether the disease-duration effect was side-specific. Secondary follow-up models regressed follow-up AMD on baseline left and right ALPS as a two-model hemisphere-specific family, with follow-up AMD modeled as log(Follow-up AMD + 1), additionally adjusting for log(Baseline AMD + 1), baseline MMD, disease duration, age, sex, and BMI. Follow-up AMD was assessed after MRI through a February 2026 telephone follow-up, not a prespecified protocol visit, so these models were interpreted as exploratory. Exploratory pooled subtype interaction tests were used to screen for heterogeneity across EM, CM, and VM; these analyses were interpreted descriptively because subtype sample sizes were small and sex counts were sparse within subtypes. Targeted clinical-confounder sensitivity checks added HADS total or ever preventive-treatment history one at a time to the main patient-only duration and follow-up models.

All tests were two-sided, and $p < 0.05$ was considered statistically significant unless otherwise specified. Analyses were performed in Python 3.13 using pandas, SciPy, statsmodels, and openpyxl.

Results

Participant characteristics

The final case-control sample consisted of 25 healthy controls and 64 pooled migraine patients. Controls and patients were similar in age (36.20 ± 9.16 vs 36.84 ± 9.52 years, p=0.770) and BMI (22.36 ± 1.53 vs 21.55 ± 2.44 kg/m², p=0.074), whereas male sex was numerically less frequent in patients (7.8% vs 24.0%, p=0.067) (Table 1). Within the migraine cohort, mean disease duration was 16.0 ± 9.7 years, baseline MMD was 10.0 ± 8.6 days, baseline AMD was 6.1 ± 7.5 days, and follow-up AMD at the February 2026 assessment was 3.4 ± 4.8 days. Patient-reported burden was also substantial (MIDAS 24.3 ± 33.1, HIT-6 59.0 ± 11.3, HADS 18.4 ± 10.5), 34 patients reported ever receiving preventive treatment, and 45 reported unilateral headache location; detailed side labels were retained for 34 patients (10 left, 7 right, 12 bilateral, 5 alternating). The cohort comprised 20 patients with EM, 24 with CM, and 20 with VM; subtype-level clinical descriptors are summarized descriptively in Supplementary Table S3.

At the unadjusted descriptive level, no ALPS metric differed significantly between controls and the pooled patient cohort. Left ALPS was 1.535 ± 0.146 in controls and 1.553 ± 0.142 in patients (descriptive p=0.601), whereas right ALPS was 1.459 ± 0.132 and 1.487 ± 0.119, respectively (descriptive p=0.376) (Table 1).

Case-control bilateral ALPS comparison

In the adjusted bilateral GEE model, patient status was not associated with ALPS (β=0.0230, 95% CI -0.0463 to 0.0923, p=0.515 for the left-sided patient-control contrast), and the patient-by-side interaction was not statistically significant (β=-0.0008, 95% CI -0.0599 to 0.0583, p=0.979) (Table 2). Side itself was significant: the right hemisphere showed a lower ALPS value than the left across the case-control dataset (β=-0.0653, 95% CI -0.1149 to -0.0156, p=0.010) (Figure 2A).

Derived contrasts showed that the right-left difference was present in both healthy controls (estimate -0.0653, p=0.010) and patients (estimate -0.0661, p<0.001). However, neither the left-sided patient-control contrast (p=0.515) nor the right-sided patient-control contrast (p=0.484) was significant. Paired within-group comparisons were consistent with the GEE results: left ALPS exceeded right ALPS in controls (paired t p=0.007; Wilcoxon p=0.008) and in patients (paired t p<0.001; Wilcoxon p<0.001) (Figure 2B).

Patient-only multivariable associations

Patient-level analyses focused on the pooled migraine cohort (n=64), where duration-sensitive variation could be examined directly while accounting for baseline attack frequency. In FDR-controlled baseline-MMD-adjusted models, longer disease duration was most clearly associated with higher ALPS difference (right-left; β=0.0053, 95% CI 0.0018 to 0.0088, p=0.003; FDR-corrected p=0.015) and lower absolute ALPS difference (β=-0.0037, 95% CI -0.0064 to -0.0011, p=0.006; FDR-corrected p=0.016). The association with lower left ALPS was directionally similar but only nominal after FDR correction (β=-0.0047, 95% CI -0.0093 to -0.0001, p=0.045; FDR-corrected p=0.076), whereas right ALPS and mean ALPS were not statistically significant (Table 3).

Table 3. Baseline-MMD-adjusted patient-only models for disease duration and hemisphere-specific follow-up AMD

Outcome	Predictor	n	β (95% CI)	P	FDR-corrected p	Adjusted R^2
Left ALPS	Duration, per year	64	-0.0047 (-0.0093 to -0.0001)	0.045	0.076	0.146
Right ALPS	Duration, per year	64	0.0006 (-0.0037 to 0.0049)	0.793	0.793	-0.002
Mean ALPS	Duration, per year	64	-0.0021 (-0.0062 to 0.0020)	0.322	0.403	0.078
ALPS difference (right-left)	Duration, per year	64	0.0053 (0.0018 to 0.0088)	0.003	0.015	0.103
Absolute ALPS difference	Duration, per year	64	-0.0037 (-0.0064 to -0.0011)	0.006	0.016	0.168
Follow-up AMD	Left ALPS	64	1.2874 (0.2576 to 2.3172)	0.014	0.029	0.515
Follow-up AMD	Right ALPS	64	0.2793 (-1.0012 to 1.5597)	0.669	0.669	0.467

Legend: Panel A shows multivariable associations between baseline ALPS metrics and disease duration in the pooled migraine cohort (n=64), adjusted for baseline MMD, age, sex, and BMI. Panel B shows the two-model hemisphere-specific follow-up family relating baseline left and right ALPS to follow-up AMD after adjustment for baseline MMD, baseline AMD, disease duration, age, sex, and BMI. Follow-up AMD was modeled as log(Follow-up AMD + 1). FDR-corrected p indicates the Benjamini-Hochberg false-discovery-rate-adjusted p value applied separately within Panel A (5 tests) and Panel B (2 tests). Adjusted R^2 values are reported for descriptive model fit only.

In the two-model hemisphere-specific secondary follow-up family, higher baseline left ALPS was associated with greater follow-up AMD assessed in February 2026 after adjustment for baseline AMD, baseline MMD, disease duration, age, sex, and BMI (β=1.2874, 95% CI 0.2576 to 2.3172, p=0.014; FDR-corrected p=0.029; Figure 4A). The corresponding right-ALPS association was not statistically significant (β=0.2793, 95% CI -1.0012 to 1.5597, p=0.669).

In the baseline-MMD-adjusted patient-only hemisphere-aware GEE, disease duration showed a significant interaction with side (β=0.0053, 95% CI 0.0024 to 0.0082, p<0.001). Side-specific contrasts demonstrated that duration was associated with lower left ALPS (β=-0.0047, 95% CI -0.0089 to -0.0006, p=0.026), whereas the association with right ALPS was not statistically significant (β=0.0006, 95% CI -0.0029 to 0.0041, p=0.741) (Table S1 and Figure 3A-B).

The coefficient summary of the continuous duration models showed the same pattern: duration was positively associated with ALPS difference and inversely associated with absolute ALPS difference after FDR correction, whereas the left-ALPS slope remained nominal (Figure 3C).

The baseline left-ALPS association with follow-up AMD was consistent across the minimally adjusted base model, subtype-adjusted refit, and baseline-MMD-adjusted main model (Figure 4B; Table S2 for subtype-adjusted estimates).

Sensitivity analyses were consistent with the same hierarchy. After additional adjustment for EM/CM/VM subtype, disease duration remained associated with higher ALPS difference (p=0.002; FDR-corrected p=0.010) and lower absolute ALPS difference (p=0.012; FDR-corrected p=0.031), whereas the left-ALPS duration coefficient remained directionally negative but did not survive FDR correction (β=-0.0049, p=0.039; FDR-corrected p=0.065). In the longitudinally separated models, baseline left ALPS remained associated with greater follow-up AMD after subtype adjustment (β=1.2951, 95% CI 0.2590 to 2.3312, p=0.014; FDR-corrected p=0.029), whereas baseline right ALPS again was not statistically significant (p=0.681). Targeted sensitivity checks adding either HADS total or ever preventive-treatment history gave the same interpretation: duration remained associated with ALPS difference and absolute ALPS difference after FDR correction, the left-ALPS duration coefficient remained nominal, and the left-ALPS follow-up AMD association remained FDR-significant (Table S2). Exploratory pooled interaction tests did not support clear EM/CM/VM heterogeneity for ALPS difference, the bilateral side-by-duration model, or the left-ALPS follow-up AMD association (Table S2). These interaction checks were interpreted by direction and uncertainty rather than as definitive subtype tests.

Discussion

Our reading is straightforward: ALPS did not behave as a simple migraine-versus-control marker in this dataset. Instead, the strongest signal was a duration-linked asymmetry pattern within the migraine cohort: longer disease duration tracked higher right-minus-left ALPS difference and lower absolute ALPS difference, consistent with less leftward asymmetry at longer duration. The single left-ALPS slope pointed in the same direction but remained nominal after FDR correction. The estimates were generated after baseline-MMD adjustment, with similar results after adding HADS total or ever preventive-treatment history.

The non-significant adjusted patient-control contrast fits within a heterogeneous cross-sectional migraine imaging literature, in which glymphatic-related metrics have ranged from null to elevated or impaired findings [7–11]. The case-control result therefore supports a limited conclusion: this cohort did not show a robust overall patient-control ALPS difference.

Another key finding is hemispheric asymmetry. Both healthy controls and patients showed lower right than left ALPS, indicating that laterality in this metric is not purely disease-generated in our cohort. This observation fits with the broader migraine literature summarized by Blum and colleagues, who emphasized that migraine lateralization is common but clinically heterogeneous [15]. In that context, hemisphere-specific analysis becomes important because longer disease duration may be associated with a weaker left-greater-than-right pattern rather than a uniform bilateral decrement.

The combination of a non-significant case-control contrast and a negatively signed disease-duration slope on the left is consistent with a duration-associated asymmetry gradient rather than a monotonic bilateral ALPS difference. This pattern remains descriptive, not mechanistic. One interpretation is that the left-greater-than-right ALPS profile was weaker among patients with longer disease duration, whereas right-sided ALPS showed little corresponding decrease. Alternative explanations include dominant-hemisphere physiology, clinical headache laterality, or technical factors such as ROI placement sensitivity and crossing-fiber bias [21].

Higher baseline left ALPS was associated with greater follow-up AMD in the two-model hemisphere-specific follow-up family. We treat this as a secondary exploratory signal: all 64 patients were reached in February 2026, but the assessment was telephone-based and not a prespecified protocol visit. The left-ALPS coefficient remained positive after adjustment for baseline AMD, disease duration, and baseline MMD, whereas the right-ALPS coefficient did not. The result motivates prospective studies with synchronized medication-use windows rather than a prognostic claim in the present data.

Together, these results indicate that hemisphere-aware duration modeling revealed patient-internal ALPS associations not captured by simple case-control status in this migraine cohort. The clearest duration-related signals resided in asymmetry metrics, not a single unilateral coefficient, supporting preservation of hemisphere information in future migraine ALPS studies. The follow-up AMD association remains secondary to this duration/asymmetry framework and mainly motivates prospective designs with synchronized clinical windows and explicitly modeled imaging-to-follow-up intervals.

This study has several strengths. It included healthy controls, complete EM/CM/VM subtype coding adjudicated by two headache specialists, hemisphere-aware modeling, standardized template-space ROI placement, and longitudinally separated follow-up information.

Several limitations define interpretation. The primary patient-versus-control analyses pooled EM, CM, and VM to preserve statistical efficiency, which may have diluted subtype-level signals, although subtype-adjusted models and exploratory pooled interaction tests did not suggest clear EM/CM/VM heterogeneity. The patient cohort also included fewer men than the control group, so sex-specific inference remains limited despite covariate adjustment. The de-identified analytical extract retained HADS total, ever preventive-treatment history, and partial headache-location information, but it did not systematically retain variables needed for a clinical-sidedness analysis, including complete headache laterality, handedness, aura status, sleep quality, medication-overuse phenotype, and treatment timing or class. HADS was used as a symptom-burden covariate rather than as a diagnostic psychiatric interview. Formal inter-rater or intra-rater repeatability statistics for ROI placement and ALPS extraction were not available. For the follow-up AMD analyses, the February 2026 assessment was telephone-based and recall-based; inter-visit treatment changes, individual imaging-to-follow-up intervals, and AMD aggregation windows were unavailable. These constraints keep mechanistic and follow-up interpretations bounded.

Conclusions

In this migraine case-control cohort, hemisphere-specific ALPS metrics revealed disease-duration associations not captured by adjusted case-control status alone. The clearest signal was a less leftward ALPS asymmetry pattern at longer disease duration, whereas the inverse association with left ALPS alone was directionally consistent but did not survive FDR correction. A secondary analysis linked baseline left ALPS with later acute medication use within a two-model hemisphere-specific follow-up family; this estimate remains exploratory because follow-up was obtained after MRI through a February 2026 telephone assessment. These results support preserving hemisphere-specific ALPS information in migraine studies and testing duration/follow-up links in prospective designs with synchronized clinical windows and systematic recording of treatment exposure and headache lateralization.

Abbreviations

ALPS
Analysis along the perivascular space
AMD
Acute medication days
ANTs
Advanced Normalization Tools
BMI
Body mass index
CI
Confidence interval
DTI
Diffusion tensor imaging
FA
Fractional anisotropy
FDR
False discovery rate
FOV
Field of view
FSL
FMRIB Software Library
GEE
Generalized estimating equation
MMD
Monthly migraine days
MRI
Magnetic resonance imaging
ROI

Region of interest
SD
Standard deviation

Declarations

Ethics approval and consent to participate

The study was approved by the Ethics Committee of the First Affiliated Hospital of Chongqing Medical University (approval No. CY2020-594). All participants provided written informed consent before enrollment and MRI examination. The present secondary analysis was additionally approved by the same Ethics Committee (approval No. 2026-0375-01). All procedures performed in studies involving human participants were in accordance with the **1964 Helsinki Declaration and its later amendments**.

Consent for publication

Not applicable.

Availability of data and materials

The de-identified analytical dataset and analysis outputs supporting this manuscript are available from the corresponding author on reasonable request, subject to institutional approval and applicable privacy restrictions.

Competing interests

Competing-interest disclosures have been finalized by all authors before submission. The authors declare that they have no known competing financial interests or personal relationships that could have appeared to influence the work reported in this paper.

Funding

This work was supported by the Chongqing Municipal Science and Health Joint Medical Research Project (2024GGXM002).

Authors' contributions

Liang Dong and Wanqun Hu contributed equally to this work.

Conceptualization: Jiying Zhou, Xiaoping Fan;

Methodology: Liang Dong, Wanqun Hu, Linyi Che;

Software: Qinlian Huang, Yuhui Xu;

Validation: Siyan Luo, Hui Li;

Analysis: Ge Tan, Liang Dong;

Investigation: Liang Dong, Wanqun Hu, Linyi Che, Qinlian Huang, Yuhui Xu, Hui Li, Ge Tan;

Resources: Jiying Zhou, Xiaoping Fan;

Data curation: Liang Dong, Wanqun Hu;

Writing – original draft: Liang Dong, Wanqun Hu;

Writing – review & editing: Jiying Zhou, Xiaoping Fan.

Acknowledgements

None.

Use of AI tools

ChatGPT (OpenAI) was used for English-language drafting and formatting support. All statistical coding, result verification, interpretation, and final content were performed and approved by the human authors.

Authors' information

Provided on the title page.

References

1. Taoka T, Masutani Y, Kawai H, et al. Evaluation of glymphatic system activity with the diffusion MR technique: diffusion tensor image analysis along the perivascular space (DTI-ALPS) in Alzheimer's disease cases. Jpn J Radiol. 2017;35(4):172-178. doi:10.1007/s11604-017-0617-z
2. Taoka T, Ito R, Nakamichi R, et al. Diffusion Tensor Image Analysis ALong the Perivascular Space (DTI-ALPS): revisiting the meaning and significance of the method. Magn Reson Med Sci. 2024;23(3):268-290. doi:10.2463/mrms.rev.2023-0175
3. Tatekawa H, Matsushita S, Ueda D, et al. Improved reproducibility of diffusion tensor image analysis along the perivascular space (DTI-ALPS) index: an analysis of reorientation technique of the OASIS-3 dataset. Jpn J Radiol. 2023;41(4):393-400. doi:10.1007/s11604-022-01370-2
4. Liu X, Barisano G, Shao X, et al. Cross-Vendor Test-Retest Validation of Diffusion Tensor Image Analysis along the Perivascular Space (DTI-ALPS) for Evaluating Glymphatic System Function. Aging Dis. 2024;15(4):1885-1898. doi:10.14336/AD.2023.0321-2
5. Zhang Y, Zhang R, Ye Y, et al. The Influence of Demographics and Vascular Risk Factors on Glymphatic Function Measured by Diffusion Along Perivascular Space. Front Aging Neurosci. 2021;13:693787. doi:10.3389/fnagi.2021.693787

6. Toriello M, González-Quintanilla V, Pérez-Pereda S, Fontanillas N, Pascual J. The potential role of the glymphatic system in headache disorders. Pain Med. 2021;22(12):3098-3100. doi:10.1093/pm/pnab137
7. Vittorini MG, Sahin A, Trojan A, et al. The glymphatic system in migraine and other headaches. J Headache Pain. 2024;25(1):34. doi:10.1186/s10194-024-01741-2
8. Lee DA, Lee HJ, Park KM. Normal glymphatic system function in patients with migraine: a pilot study. Headache. 2022;62(6):718-725. doi:10.1111/head.14320
9. Zhang X, Wang W, Bai X, et al. Increased glymphatic system activity in migraine chronification by diffusion tensor image analysis along the perivascular space. J Headache Pain. 2023;24(1):147. doi:10.1186/s10194-023-01673-3
10. Cao Y, Huang M, Fu F, et al. Abnormally glymphatic system functional in patients with migraine: a diffusion kurtosis imaging study. J Headache Pain. 2024;25(1):118. doi:10.1186/s10194-024-01825-z
11. Wu CH, Chang FC, Wang YF, et al. Impaired Glymphatic and Meningeal Lymphatic Functions in Patients with Chronic Migraine. Ann Neurol. 2024;95(3):583-595. doi:10.1002/ana.26842
12. Ren X, Wang H, He Y, et al. Impaired meningeal lymphatic drainage correlates with headache intensity in episodic migraine. J Headache Pain. 2025;26:265. doi:10.1186/s10194-025-02211-z
13. Cai X, Sun W, Cai M, et al. Impaired glymphatic function contributes to high-frequency attacks in patients with episodic migraine. J Headache Pain. 2025;26:132. doi:10.1186/s10194-025-02070-8
14. Ornello R, Salfi F, Vittorini MG, et al. The potential role of sleep quality in the relationship between glymphatic function and migraine frequency: Insights from a cross-sectional study. Headache. 2025 Aug 19. doi:10.1111/head.15019
15. Blum ASS, Riggins N, Loder EW, et al. Left- vs right-sided migraine: a scoping review. J Neurol. 2023;270(6):2938-2949. doi:10.1007/s00415-023-11609-1
16. Sprouse Blum AS, DaSilva LA, Greenberg MD, Nissenbaum AJ, Shapiro RE, Littenberg B. Comparison of migraine with left- versus right-sided headache: A cross-sectional study. Headache. 2024;64(3):259-265. doi:10.1111/head.14689
17. Ashina M, Terwindt GM, Al-Karagholi MAM, de Boer I, Lee MJ, Hay DL, et al. Migraine: disease characterisation, biomarkers, and precision medicine. Lancet. 2021;397(10283):1496-1504. doi:10.1016/S0140-6736(20)32162-0
18. Burch RC, Buse DC, Lipton RB. Migraine: Epidemiology, burden, and comorbidity. Neurol Clin. 2019;37(4):631-649. doi:10.1016/j.ncl.2019.06.001
19. von Elm E, Altman DG, Egger M, Pocock SJ, Gøtzsche PC, Vandenbroucke JP; STROBE Initiative. The Strengthening the Reporting of Observational Studies in Epidemiology (STROBE) statement: guidelines for reporting observational studies. PLoS Med. 2007;4(10):e296. doi:10.1371/journal.pmed.0040296
20. Headache Classification Committee of the International Headache Society (IHS). The International Classification of Headache Disorders, 3rd edition. Cephalalgia. 2018;38(1):1-211.

doi:10.1177/0333102417738202

21. Georgiopoulos C, Werlin A, Lasic S, et al. Diffusion tensor imaging along the perivascular space: the bias from crossing fibres. Brain Commun. 2024;6(6):fcae421. doi:10.1093/braincomms/fcae421

Figures

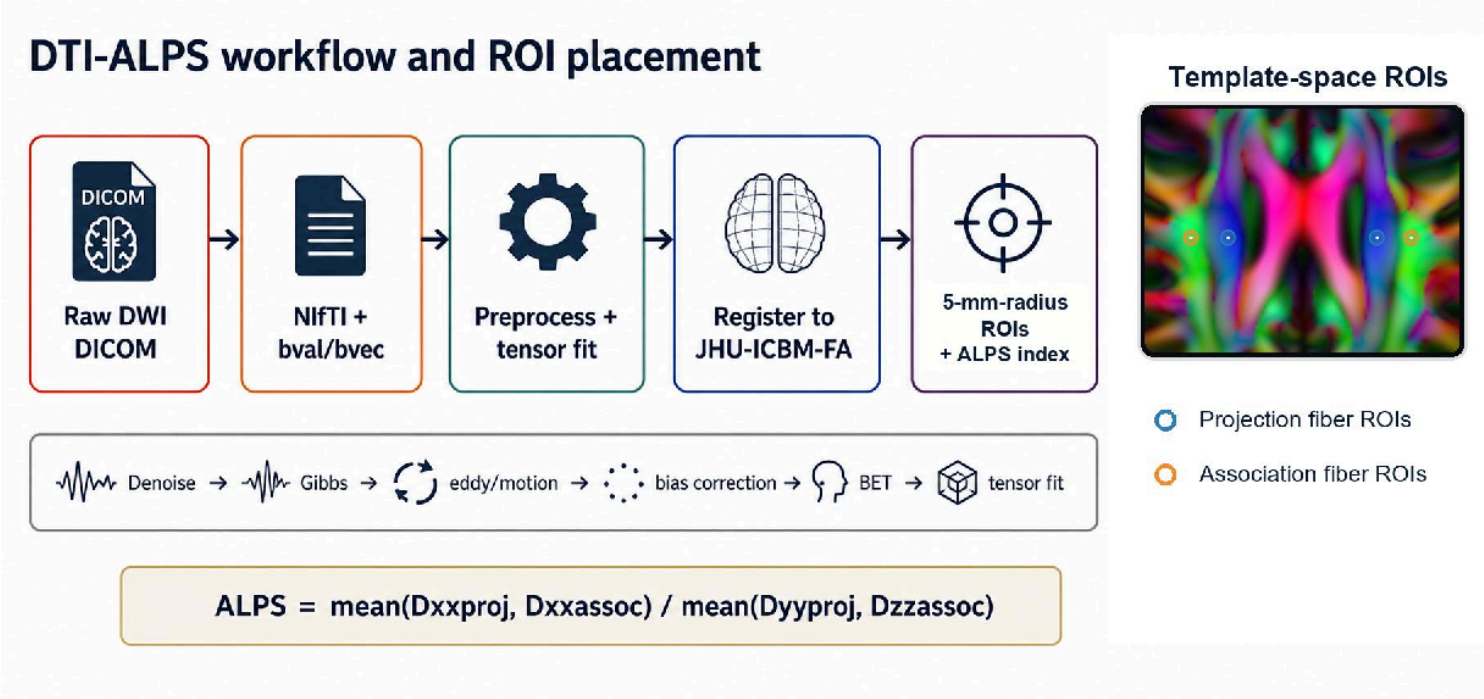


Figure 1

DTI-ALPS workflow and ROI placement

This figure summarizes DTI-ALPS preprocessing, 5-mm-radius template-space ROI placement, and the ALPS formula; blue and orange markers indicate projection- and association-fiber ROI centers, respectively.

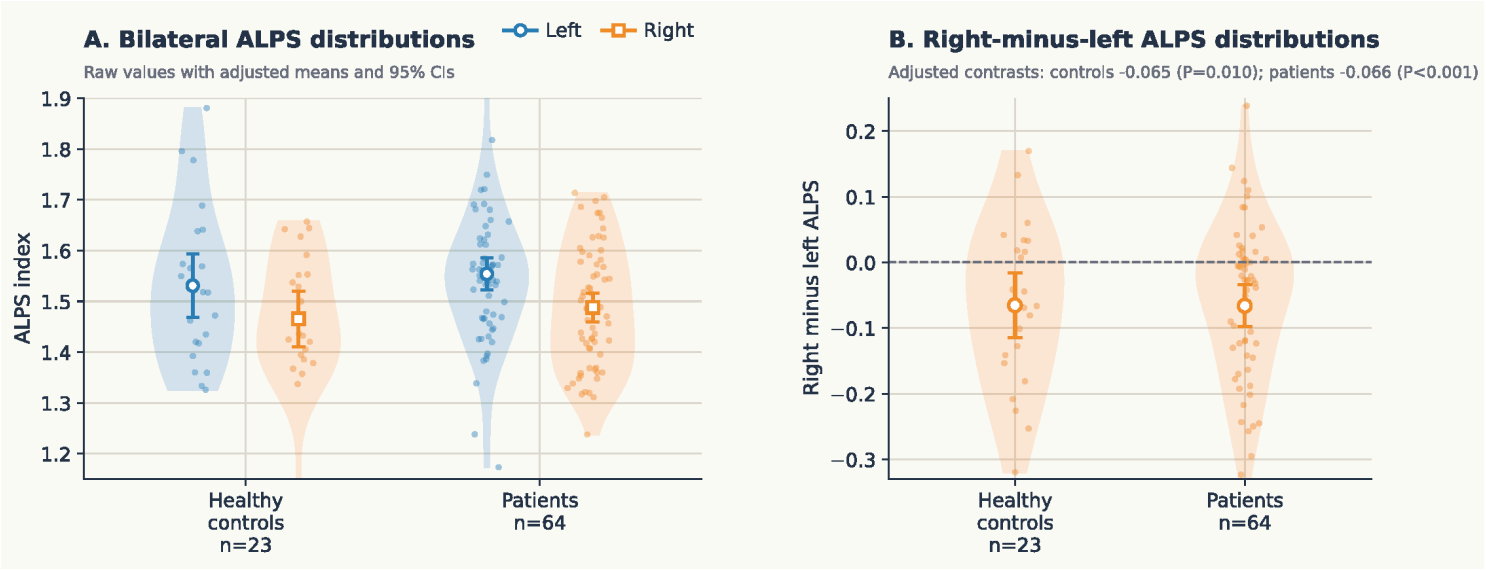


Figure 2

Case-control ALPS profile

Panel A shows BMI-complete raw left and right ALPS distributions with adjusted mean and 95% confidence interval overlays from the bilateral GEE model adjusted for age, sex, and BMI. Panel B shows BMI-complete raw right-minus-left ALPS distributions with adjusted derived contrast overlays; negative values indicate higher left than right ALPS. The displayed complete-case set includes 23 controls and 64 patients for the BMI-adjusted case-control model.

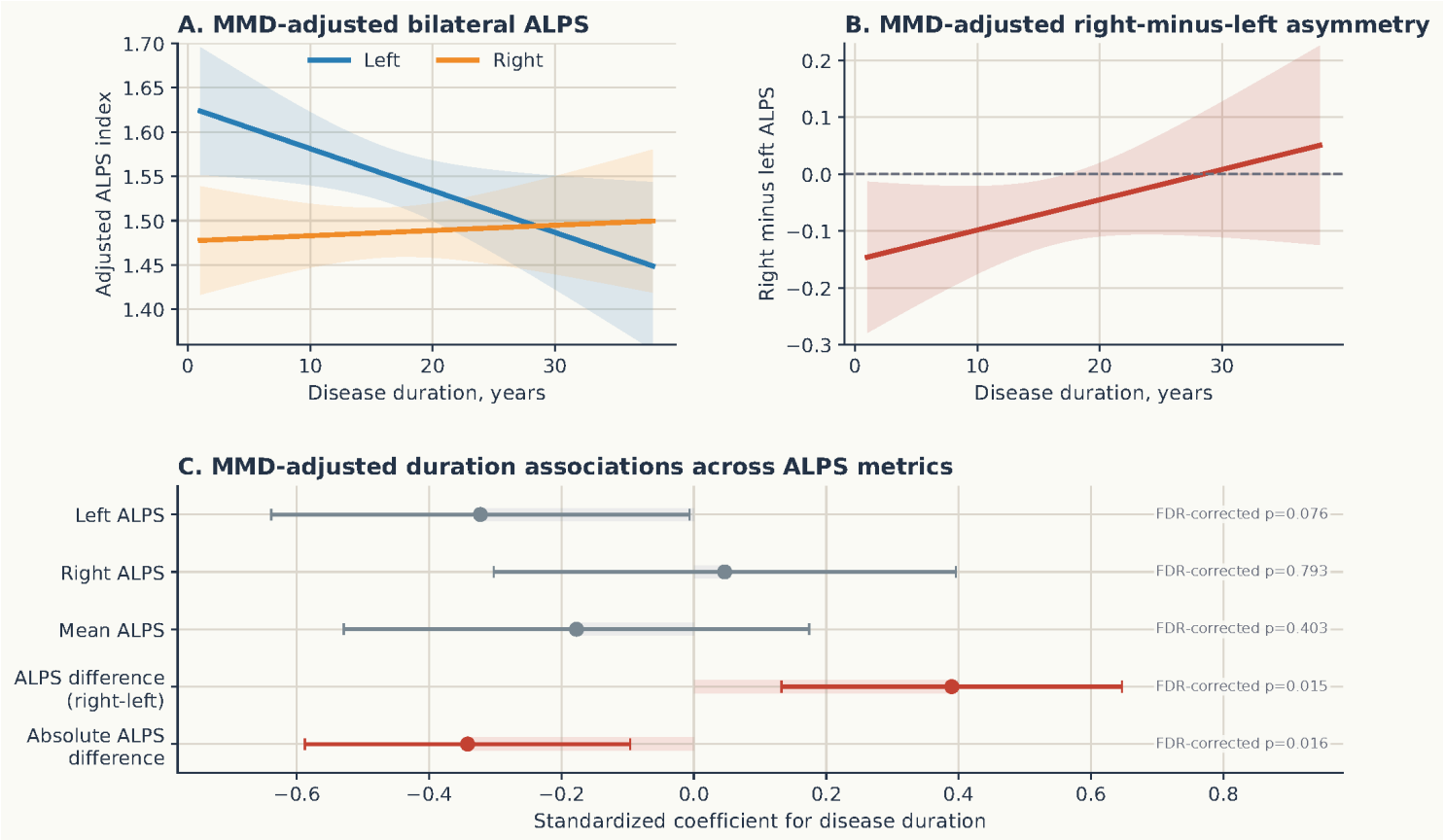


Figure 3

Disease-duration-associated ALPS asymmetry

Panel A shows model-predicted left and right ALPS values across disease duration from the patient-only hemisphere-aware GEE adjusted for baseline MMD, age, sex, and BMI, with shaded 95% confidence bands. Panel B shows the corresponding predicted right-minus-left ALPS difference across duration, where higher values indicate a less leftward asymmetry pattern. Panel C shows standardized coefficients and 95% confidence intervals from baseline-MMD-adjusted patient-only duration models across ALPS metrics; these correlated metrics are interpreted as complementary displays of one duration/asymmetry family, and FDR-corrected p values are shown for the displayed model family.

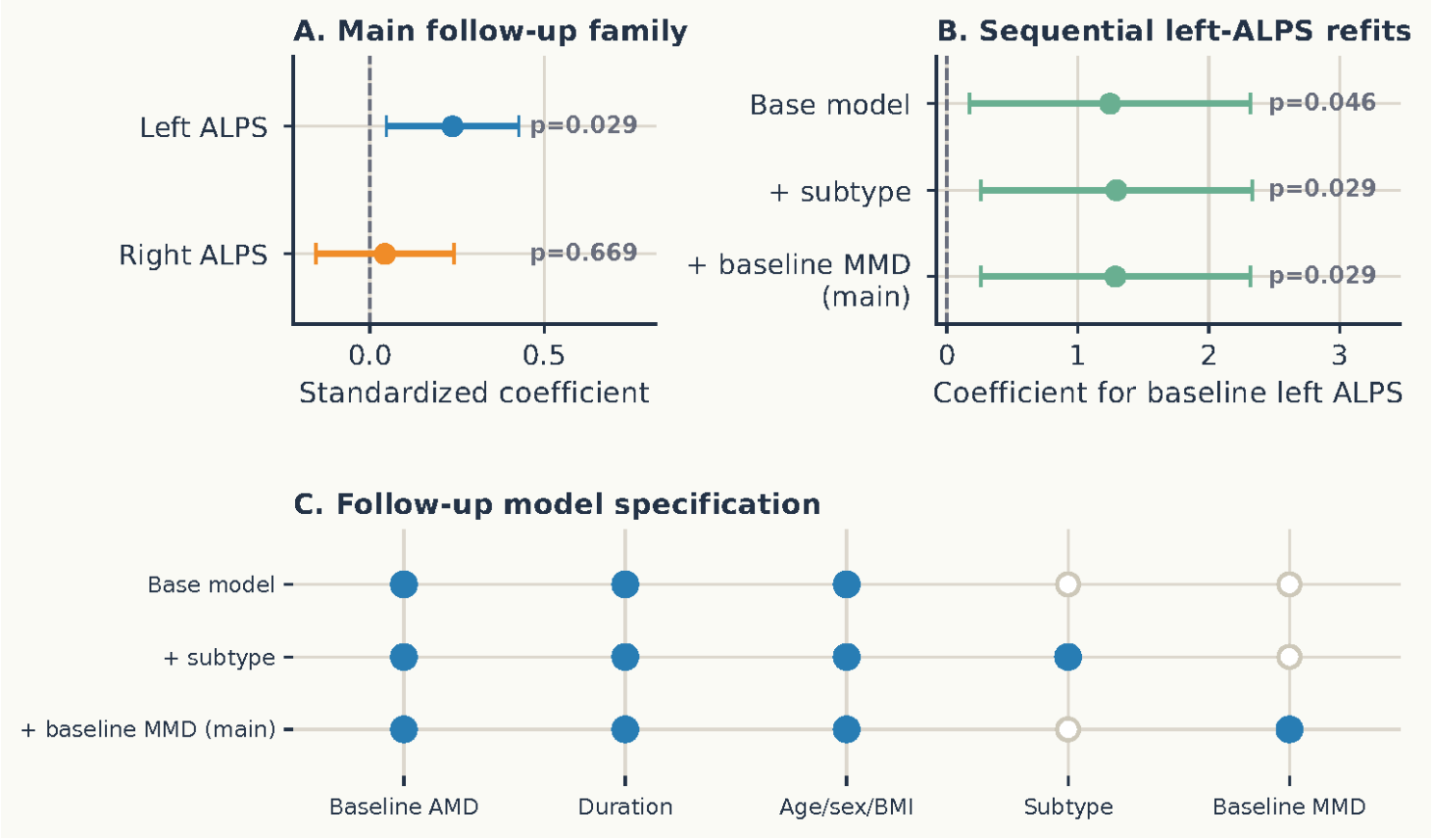


Figure 4

Secondary exploratory follow-up AMD association

Panel A shows standardized coefficients and 95% confidence intervals from the secondary exploratory two-model hemisphere-specific follow-up family. Baseline left and right ALPS, log(Baseline AMD + 1), baseline MMD, disease duration, and log(Follow-up AMD + 1) were z-transformed before refitting HC3-robust models adjusted for age, sex, and BMI; positive coefficients indicate that higher baseline metric values were associated with greater follow-up AMD. Panel B shows sequential left-ALPS refits: the minimally adjusted base model, the subtype-adjusted refit, and the baseline-MMD-adjusted main model,

with coefficients shown on the log(Follow-up AMD + 1) scale. Panel C summarizes model specification: filled circles indicate covariates included in each refit, and open circles indicate covariates not included in that model. Point labels in Panels A and B are FDR-corrected p values; FDR correction was applied within the left/right ALPS follow-up family. All follow-up models used n=64 with complete follow-up ascertainment.

Supplementary Files

This is a list of supplementary files associated with this preprint. Click to download.

- ALPSTJHPsupplementarytables.docx
- ALPSTJHPSTROBEchecklist.docx